ELSEVIER

www.elsevier.nl/locate/jorganchem

Journal of Organometallic Chemistry 586 (1999) 125–137

Journal of Organometallic Chemistry

Synthesis of Rh(I) and Ir(I) metal complexes with the first two chiral dithiolate ligands derived from carbohydrates

Oscar Pàmies, Gemma Net, Aurora Ruiz *, Carles Bo, Josep Maria Poblet, Carmen Claver

Departament de Química Física i Inorgànica, Universitat Rovira i Virgili, Pl. Imperial Tàrraco 1, E-43005 Tarragona, Spain

Received 23 February 1999; received in revised form 24 April 1999

Abstract

New chiral dithiol compounds 1,2-O-isopropylidene-3,5-dithiol-α-D-ribofuranose $RiSSH_2$ and 1,2-O-isopropylidene-3,5-dithiol-α-D-xylofuranose $XySSH_2$ and their chiral dithiolate olefinic Rh(I) and Ir(I) complexes $[M_2(\mu\text{-RiSS})(cod)_2]$ (M = Rh **1**, Ir **3**) and $[M_2(\mu\text{-XySS})(cod)_2]$ (M = Rh **2**, Ir **4**) were synthesized and characterized. The Rh(I) complexes reacted with CO to give the corresponding binuclear tetracarbonyls $[Rh_2(\mu\text{–RiSS})(CO)_4]$ (**5**) and $[Rh_2(\mu\text{-XySS})(CO)_4]$ (**6**), which reacted with two equivalents of PPh_3 to form mixed carbonyl-phosphine complexes $[Rh_2(\mu\text{-RiSS})(CO)_2(PPh_3)_2]$ (**7**) and $[Rh_2(\mu\text{-XySS})(CO)_2(PPh_3)_2]$ (**8**). The structures of $[Rh_2(\mu\text{-RiSS})(CO)_4]$ (**5**) and the two possible conformers of $[Rh_2(\mu\text{-XySS})(CO)_4]$ (**6a**) and (**6b**) were optimized and their relative stability determined by theoretical methods based on density functional theory (DFT). An interaction between one Rh atom and the oxygen atom of the ring was found in the most stable conformer of $[Rh_2(\mu\text{-XySS})(CO)_4]$. The complexes $[Rh_2(\mu\text{-RiSS})(cod)_2]$ (**1**) and $[Rh_2(\mu\text{-XySS})(cod)_2]$ (**2**) were used as catalytic precursors in the hydroformylation of styrene. The results suggest that mononuclear rhodium hydride carbonyl species are responsible for the catalytic activity.

Keywords: Rhodium(I); Iridium(I); Chiral dithiolates; Carbohydrate derivatives; DFT molecular orbital calculations

1. Introduction

In recent decades the efficiency of asymmetric homogeneous catalysis with chiral organometallic complexes in the synthesis of optical pure drugs, agrochemicals, flavors or fragrancies has meant that great efforts have been made to design new chiral ligands [1]. One of the simplest methods of obtaining chiral substances is the transformation or derivatization of readily available natural chiral compounds (the so-called chiral pool). Some carbohydrates are particularly advantageous because they are inexpensive compounds [2]. Thus, in the last three decades, carbohydrates have been used as starting material in the synthesis of chiral auxiliaries for asymmetric synthesis [3]. Nevertheless, despite the accessibility of carbohydrate synthons, the full potential of the carbohydrate chiral pool for providing chiral ligands has hardly been exploited [4]. Most chiral ligands with carbohydrates as building blocks are P-ligands derived from glucose but there are also examples derived from other monosaccharides or other carbohydrates [4,5]. Some of them have given very high enantioselectivities in asymmetric catalysis [5–9] and have been applied in industry to synthesize L-DOPA [10].

The S-ligands derived from carbohydrates have been studied much less than their P-counterparts. To the best of our knowledge, the only contributions to this area study compounds derived from glucose, one of which is a ligand with only sulfur as donor atom [11], while the rest are P–S ligands [12–14].

In homogeneous catalysis, sulfur ligands are efficient for reactions such as the hydroformylation or hydrogenation of olefines [15]. This feature, together with their advantages over phosphorous ligands (less expensive, less toxic and less oxidisable) [16] is an incentive for further investigation in this field.

Here we report the synthesis of the first dithiolate ligands with a backbone derived from carbohydrates. Two epimer ligands derived from ribofuranose and

* Corresponding author. Fax: +34-977-559563.
E-mail address: aruiz@quimica.urv.es (A. Ruiz)

0022-328X/99/$ - see front matter
PII: S0022-328X(99)00251-X

xylofuranose, respectively (Scheme 1) and their corresponding Rh(I) and Ir(I) complexes have been synthesized. Following our previous work in hydroformylation catalyzed by dithiolate rhodium complexes [17], we also report the results obtained in the hydroformylation of styrene by using rhodium complexes with the new dithiolate ligands as precatalysts.

2. Results and discussion

2.1. Synthesis of chiral dithiols $RiSSH_2$ and $XySSH_2$

$RiSSH_2$ and $XySSH_2$ were prepared according to Scheme 1. The bisthioacetate ribose derivative **V** has already been described in the literature starting from the corresponding ditosylate [18]. All attempts to reproduce this reaction led mainly to decomposition products or, in milder conditions, to the substitution of only one of the tosyl groups. The bisthioacetate ribose and xylose derivatives **V** and **VI** were finally obtained from the corresponding ditriflates **III** and **IV**. The yield obtained in the case of **V** was much lower because the nucleofilic attack took place through the most sterically hindered face. This unfavorable kinetics led to secondary reactions, principally the elimination of the triflyl group. The dithiol derivatives $RiSSH_2$ and $XySSH_2$ were easily obtained by reacting **V** and **VI** with the exchange resin IRA-420 in methanol. $NaBH_4$ in ethanol (75%) was also able to reduce the thioacetate groups to thiol groups though with lower yields.

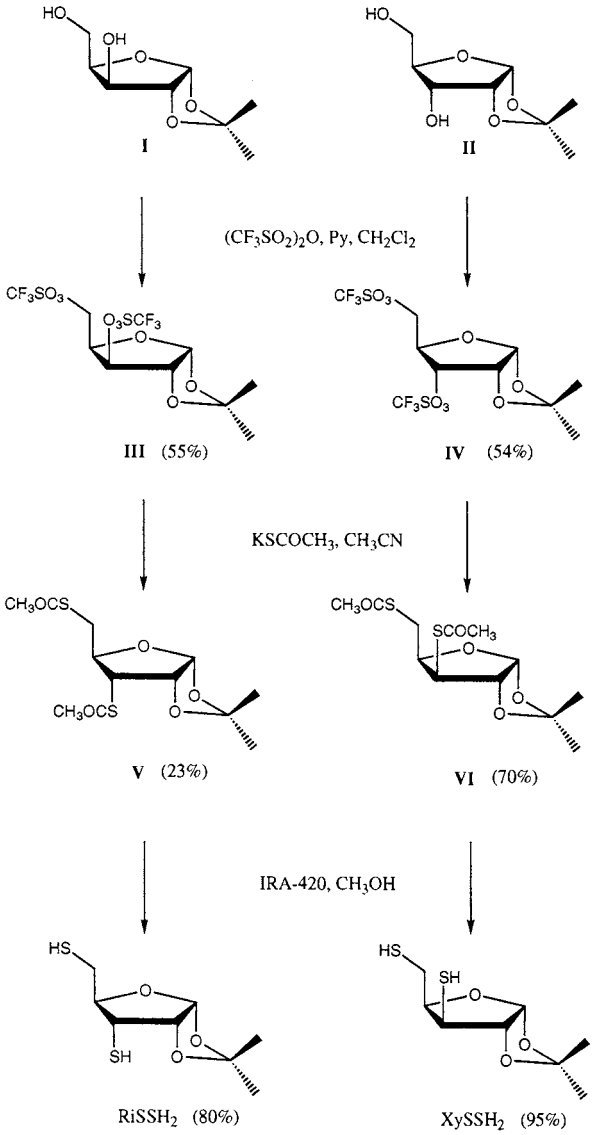

Scheme 1. Synthesis of H_2RiSS and H_2XySS.

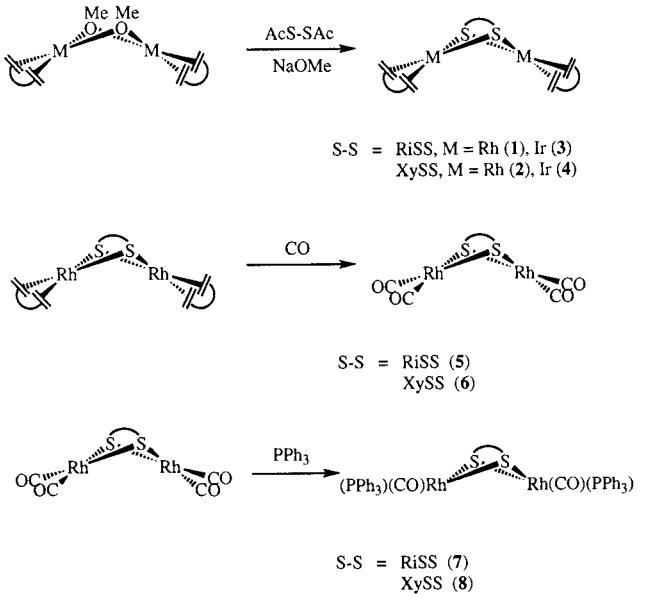

Scheme 2. Synthesis of the complexes with XySS and RiSS (**1**–**8**).

2.2. Synthesis of the dithiolate complexes

2.2.1. Olefinic Rh(I) and Ir(I) complexes

The $[Rh_2(\mu\text{-RiSS})(cod)_2]$ (**1**) and $[Rh_2(\mu\text{-XySS})(cod)_2]$ (**2**) red complexes were synthesized easily from the bisthioacetate derivatives, **V** and **VI**, and $[Rh(\mu\text{-OMe})(cod)]_2$ with sodium methoxide acting as catalyst (Scheme 2). Synthesis from the corresponding dithiols $RiSSH_2$ and $XySSH_2$ and $[Rh(\mu\text{-OMe})(cod)]_2$ gave similar yields. Though both compounds are air-stable solids, they decompose slowly in solution if not kept under nitrogen. Complex **1** is by far the least stable. Dithiolate Rh(I) complexes are known to be dinuclear or tetranuclear [19]. The FAB mass spectra for **1** and **2** show the heaviest peaks at m/z 642. This suggests that both compounds are dinuclear. The anomeric proton of **1** (5.55 ppm) appears at higher field than the anomeric proton of $RiSSH_2$ (5.82 ppm), as expected from the coordination to the metal [20], whereas the anomeric

proton of **2** (6.34 ppm) appears further downfield than $XySSH_2$ (5.93 ppm). Below we shall discuss this shift downfield with coordination.

The $[Ir_2(\mu\text{-RiSS})(cod)_2]$ (**3**) and $[Ir_2(\mu\text{-XySS})(cod)_2]$ (**4**) brown complexes were synthesized analogously to the parent rhodium compounds (Scheme 2). Their FAB mass spectra suggest that the iridium complexes **3** and **4** are dinuclear. They are relatively air stable in the solid state but they are very unstable in solution even under nitrogen atmosphere, which meant that their reactivity could not be studied. They could not be characterized by ^{1}H-NMR, even at low temperatures, because of the presence of peaks that were too wide.

2.2.2. Rh (I) carbonylic complexes

Bubbling CO through solutions of **1** and **2** in methylene chloride afforded the corresponding tetracarbonylic compounds $[Rh_2(\mu\text{-RiSS})(CO)_4]$ (**5**) and $[Rh_2(\mu\text{-XySS})(CO)_4]$ (**6**) (Scheme 2). All attempts to isolate these complexes failed because of their high solubility in organic solvents. In contrast to their olefinic precursors **1** and **2**, solutions of the carbonylic compounds **5** and **6** are air stable over long periods (weeks).

All the dithiolate-bridged tetracarbonyl Rh(I) or Ir(I) complexes that have been structurally characterized by X-ray [21] or IR [17e,19] spectrometry are dinuclear. The IR spectra of methylene chloride solutions of **5** and **6** show four stretching carbonyl frequencies near 2000 cm^{-1} and suggest that these complexes are also dinuclear (see the corresponding section).

Like the olefinic precursors, the ^{1}H-NMR spectra of **5** and **6** show the same pattern. Again, the anomeric proton of **5** (5.66 ppm) appears further upfield than the anomeric proton of $RiSSH_2$ (5.82 ppm), as expected from the coordination to the metal, whereas the anomeric proton of **6** (6.16 ppm) appears further downfield than $XySSH_2$ (5.93 ppm).

2.2.3. Theoretical structures for $[Rh_2(RiSS)(CO)_4]$ and $[Rh_2(XySS)(CO)_4]$

Much interest has recently been shown in methods based on density functional theory (DFT) as an alternative to ab initio schemes for organometallic complexes [22]. Initial geometries were generated by means of molecular mechanics calculations for complexes **5** and **6** as well as for olefinic complexes **1** and **2**. During this study, it was realized that whilst the coordinated $RySS^{2-}$ ligand (complexes **1** and **5**) can only have one conformation, $XySS^{2-}$ complexes can be present as two conformers, **2a** and **2b** for olefinic complexes and **6a** and **6b** for carbonylic complexes. The bridging dithiolate ligands of conformers **1**, **5**, **2b** and **6b** have a similar conformation, but it is noteworthy that in conformers **2a** and **6a** the $XySS^{2-}$ ligand bends in such a way that the oxygen from the sugar ring is above one of the rhodium atoms. Full geometry optimizations at the DFT level were carried out for **5** and the two conformers of **6**. The optimized structures and their relative energies are shown in Fig. 1. Their most representative intramolecular bond distances and angles are summarized in Table 1. From these results it can be concluded that the most stable conformer for complex **6** is **6a**.

The three conformers can be described as bent double square–planar structures. The difference between the torsion angle (RhS_2Rh) and the dihedral angle between the coordination planes (the metals are not included) suggests a slightly distorted square planar coordination around each rhodium atom. The dihedral angles between the coordination planes for the three conformers are in the range from 127 to 129° and are slightly larger than the values reported for other dinuclear dithiolate-bridged Rh complexes [17e,19a,21,23]. As expected from the large dihedral angles, the Rh–Rh distances in the three conformers are longer than the ones reported for the above mentioned compounds. These distances are outside the accepted range for metal–metal interactions in these kinds of compound, 2.617–2.796 Å [24]. The Rh–Rh distances in **5** and **6b** are practically identical, probably due to the similar conformation of the dithiolate ligand in these two conformers, and shorter than the Rh–Rh distance in **6a**. No striking features can be observed in the bond distances between the metal and the donor atoms. The Rh–S bond distances (average 2.405, 2.394 and 2.393 Å) are similar to those reported for other dithiolate-bridged Rh complexes [17e,19,21,23]. The Rh–C bond distances (average 1.865, 1.864 and 1.867 Å) are close to those of other dicarbonyl rhodium complexes [21].

The intramolecular distance between the sugar ring oxygen and one of the rhodium atoms in **6a** is only 2.840 Å at the local level and 2.982 at BP86 level, which suggests a weak interaction between the two atoms. According to the theory of atoms in molecules (AIM), the presence of a bond critical point in the charge density distribution linking two nuclei at the equilibrium geometry is a necessary and sufficient condition for the existence of a bond [25]. Such a bond critical point could be characterized in both computed density distributions of **6a** between the ring O and the Rh nuclei. The same analysis was made between the two metal atoms. The absence of a bond critical point indicates the absence of a metal–metal interaction as suggests the intermetal distance.

On the basis of the structures obtained for **6a** and **6b**, the ^{1}H-NMR shift downfield observed for the anomeric proton of **2** and **6** upon coordination can be interpreted by the anisotropic effect of the cod double bond in **2a** and the triple bond of one of the carbonyls in conformer **6a**, because both ligands are very near the anomeric proton in this ligand conformation. Between 90 and −80°C, the ^{1}H-NMR spectra of **2** and **6** did not change, thus indicating that the only conformers detected were **2a** and **6a**.

It should be pointed out that for this kind of complexes the inexpensive molecular mechanics calculations (MM) give quite good results. Calculated MM structures for **5**, **6a** and **6b** are not very different from those computed from DFT calculations (the differences in bond angles and distances are often less than 0.5% and never more than 2%). MM calculations were also able to show that conformer **6b** has greater energy than **6a**.

2.2.4. Theoretical IR spectrum in the carbonylic region for $[Rh_2(XySS)(CO)_4]$

The structures of $[Rh_2(RiSS)(CO)_4]$ (**5**) and $[Rh_2(XySS)(CO)_4]$ (**6**) were optimized assuming that they were dinuclear. The presence of four bands (Fig. 2) in the carbonyl region of their IR spectra (eight bands would be expected for a tetranuclear compound) and the dinuclearity found in all solved crystal structures of similar compounds [21] suggested this structure. In order to confirm this, the IR spectra in the carbonylic region of these compounds were further studied. For C_{2v} symmetric bisthiolate-bridged dicarbonyl Rh or Ir complexes, Poilblanc and Kalck studied the relative intensity of the three expected bands (A_1, B_1 and B_2) as a function of θ [26]. The θ angle is the dihedral angle between the planes of the CO groups of the two $Rh(CO)_2$ moieties. This study cannot be applied in our case because the asymmetry of the dithiolate bridging ligand lowers the symmetry of the complex to C_1. The shoulder observed in the spectra of **5** and **6** at lower energies is a fourth band (A_2 in a C_{2v} symmetry) which is not active for a C_{2v} symmetry but which becomes active for a C_1 symmetry. The intensity of this band is much higher for complex $[Rh_2(XySS)(CO)_4]$ than for $[Rh_2(RiSS)(CO)_4]$. This agrees with the 'higher asymmetry' of the XySS compound due to the Rh–O interaction in only one of the $Rh(CO)_2$ groups.

The IR spectrum in the carbonylic region for one of these complexes, $[Rh_2(XySS)(CO)_4]$, was theoretically calculated using the DFT methodology at the LDA

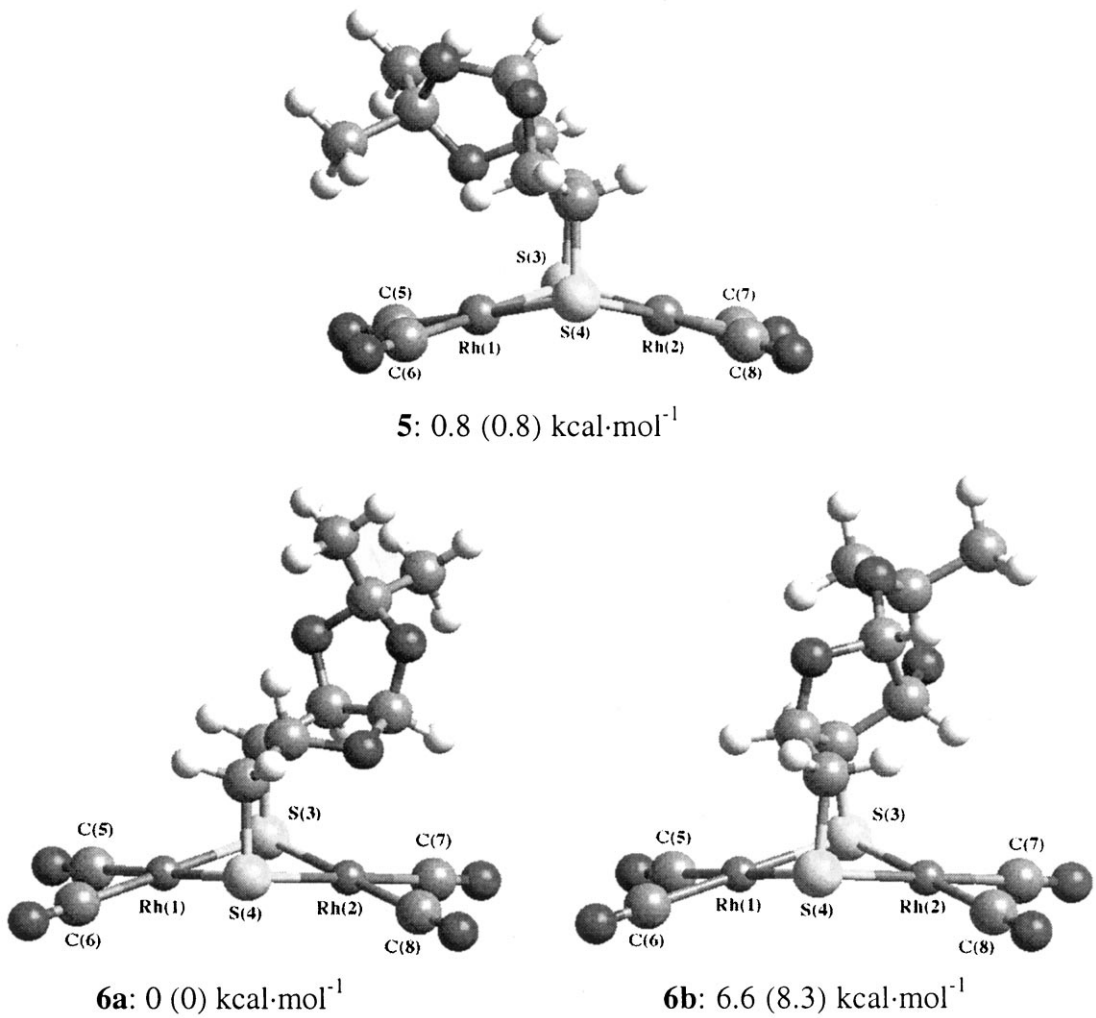

Fig. 1. Calculated structures of $[Rh_2(\mu\text{-}RiSS)(CO)_4]$ (**5**) and $[Rh_2(\mu\text{-}XySS)(CO)_4]$ (**6a** and **6b**) with their relative energies at the non-local level (values at the local level in parentheses).

Table 1
Selected geometrical parameters for $[Rh_2(\mu\text{-RiSS})(CO)_4]$ (**5**) and the two conformers of $[Rh_2(\mu\text{-XySS})(CO)_4]$ (**6a** and **6b**) calculated at the non local level. Values obtained at the LDA level are shown in parentheses [a]

	5	6a	6b
Bond lengths (Å)			
Rh(1)–Rh(2)	3.252 (3.169)	3.295 (3.202)	3.267 (3.168)
Rh(1)–S(3)	2.455 (2.405)	2.441 (2.386)	2.447 (2.391)
Rh(1)–S(4)	2.474 (2.415)	2.439 (2.387)	2.450 (2.392)
Rh(2)–S(3)	2.446 (2.398)	2.453 (2.398)	2.442 (2.390)
Rh(2)–S(4)	2.458 (2.400)	2.459 (2.405)	2.457 (2.398)
Rh(1)–C(5)	1.892 (1.864)	1.897 (1.867)	1.897 (1.867)
Rh(1)–C(6)	1.891 (1.863)	1.895 (1.866)	1.896 (1.866)
Rh(2)–C(7)	1.895 (1.867)	1.887 (1.859)	1.897 (1.868)
Rh(2)–C(8)	1.895 (1.866)	1.891 (1.864)	1.899 (1.869)
$\theta(RhS_2Rh)$ [b]	126.8 (127.4)	128.5 (129.0)	126.9 (129.0)
Bond angles (°)			
ϕ [c]	128.7(129.4)	127.6(128.1)	128.1(129.4)
C(5)–Rh(1)–C(6)	93.2 (93.7)	93.7 (94.0)	93.3 (93.3)
C(7)–Rh(2)–C(8)	93.8 (93.7)	92.9 (93.2)	93.55 (93.6)
S(3)–Rh(1)–S(4)	84.3 (84.7)	83.7 (84.8)	83.6 (85.6)
S(3)–Rh(2)–S(4)	84.8 (84.1)	83.0 (84.7)	83.6 (85.6)
Rh(1)–S(3)–Rh(2)	83.1 (84.0)	84.6 (83.0)	83.8 (82.6)
Rh(1)–S(4)–Rh(2)	82.5 (83.8)	84.5 (82.8)	83.5 (82.3)

[a] Distances in Å and angles in °.
[b] θ: torsion angle.
[c] ϕ: dihedral angle between the two mean planes containing the four coordinated atoms (C,C,S,S).

level. The frequencies of the experimental and calculated stretching CO bands are listed in Table 2. The calculated values are different from the experimental values by 0.8–2.4% and these differences are similar to those found for other carbonylic compounds [27]. $[Rh_2(S\text{-}(CH_2)_3S)(CO)_4]$ is a similar compound with a symmetric dithiolate for which the presence and intensities of three carbonyl bands in the IR suggests a dinuclear structure [19a]. The same calculation was carried out for this compound (Table 2). The differences between experimental and calculated frequencies were very similar to those found with $[Rh_2(XySS)(CO)_4]$. In summary, the similarity of the experimental and theoretical IR frequencies is further proof of the dinuclearity of these complexes.

2.2.5. Rh(I) mixed carbonyl–phosphine complexes

The complexes $[Rh_2(\mu\text{-RiSS})(CO)_4]$ (**5**) and $[Rh_2(\mu\text{-XySS})(CO)_4]$ (**6**) react at room temperature with two equivalents of PPh_3 to form the orange species $[Rh_2(\mu\text{-RiSS})(CO)_2(PPh_3)_2]$ (**7**) and $[Rh_2(\mu\text{-XySS})(CO)_2(PPh_3)_2]$ (**8**), which are air stable in the solid state (Scheme 2). These mixed dithiolate bridged complexes are known to be di- or tetranuclear depending on the dithiolate bridge [17c,19b]. The fact that the heaviest ion was at 1006 in the FAB mass spectra suggested that these complexes were dinuclear. The stoichiometry $[Rh_2(\mu\text{-SS})(CO)_2(PPh_3)_2]$, where μ-SS is an asymmetric dithiolate ligand, allows the four molecular isomeric structures depicted in Fig. 3. In the case of **8**, since the coordinated dithiolate ligand $XySS^{2-}$ can be present in two different conformations, the number of possible isomers increases to eight. The ^{31}P-NMR spectrum for both complexes had eight doublets which suggested that four possible structural isomers for this stoichiometry were present in solution for **7** and **8** but in different proportions (all the possible isomers for **7** and four of the eight possible isomers for **8**). IR spectra in solution of **7** and **8** show three broad bands in the metal carbonyl region, between 1950 and 2025 cm^{-1}, which confirm the presence of different isomers in solution.

In contrast, solid state IR spectra for these complexes show a single broad band in this region at 1967 and 1965 cm^{-1}, respectively. *Trans*-$[Rh_2(\mu\text{-SS})(CO)_2(PPh_3)_2]$ complexes with symmetrical dithiolate bridges have two very close bands in the carbonylic area with relative intensities 4.7:10, which sometimes can be seen as a single broad band [26,28]. Thus, the IR spectra of **7** and **8** suggest that these compounds are present in the solid state only as the *trans* isomers. In $[Rh_2(\mu\text{-SS})(CO)_2(PPh_3)_2]$ complexes there is often only one isomer in the solid state (*cis* or *trans*) and two isomers in solution [26,28,29].

In the ^{1}H-NMR spectra of **7** and **8** there are two groups of signals for the dithiolate protons. In **7** the chemical shifts are very similar whereas in **8** they are significantly different. Thus, the anomeric proton appears at 6.29 ppm for the major isomers and at 4.89 ppm for the minor isomers of **8**. Molecular mechanics calculations were carried out for complex **8**. When triphenylphosphine enters the L_4 position (Fig. 3), due to steric hindrance, the puckered conformation of the coordinated ligand $XySS^{2-}$ (in which the ring oxygen is above one of the rhodium atoms) is not possible. This reduces the number of possible structures for **8** from eight to six. The relative strain energies for the six possible isomers of **8** present in solution are listed in Table 3. These results show that the strain energy of the isomers depends on the conformation of the bridging ligand as observed for the other $XySS^{2-}$ compounds **2** and **6**. Again, the most stable isomers are those with the ring oxygen above one of the rhodium atoms (conformation a). Only when PPh_3 enters the L_4 position is this conformation no longer possible and the conformation of the ligand becomes more extended (b). Thus, the four isomers in the ^{31}P-NMR spectrum are the first four in Table 3 and the two groups of isomers seen in ^{1}H-NMR correspond to the two possible geometries of the ligand in the four possible isomers.

The two conformations account for the considerable differences in chemical shifts between the two groups of signals for the dithiolate protons in ^{1}H-NMR. The major isomers (with the lowest strain energy) are the two isomers with the bent conformation of the ligand (conformation a), that is to say, in which the anomeric proton is affected by the anisotropic currents of the carbonyl ligand (H1: 6.29 ppm), and the minor isomers are the two in which the ligand has conformation b and PPh_3 in L_4. (H1: 4.89 ppm).

2.3. Hydroformylation of styrene

Asymmetric hydroformylation has attracted much attention because of its potential as a synthetic tool for preparing of enantiomerically pure aldehydes, which are very important not only as precursors for biologically active compounds but also for new materials such as biodegradable polymers and liquid crystals.

Table 4 shows the results of the hydroformylation of styrene with the catalyst precursors **1** and **2** in the absence of phosphorous ligands.

The catalyst precursor $[Rh_2(\mu\text{-XySS})(cod)_2]$ (**2**) is not active at 20 bar and 75°C and is only slightly active at 30 bar (entries 1,2). Although the catalytic activity of **2** increases with time, its regioselectivity decreases, until it disappears (entries 1,2). The dependence of activity and regioselectivity on time indicates a change in the active species.

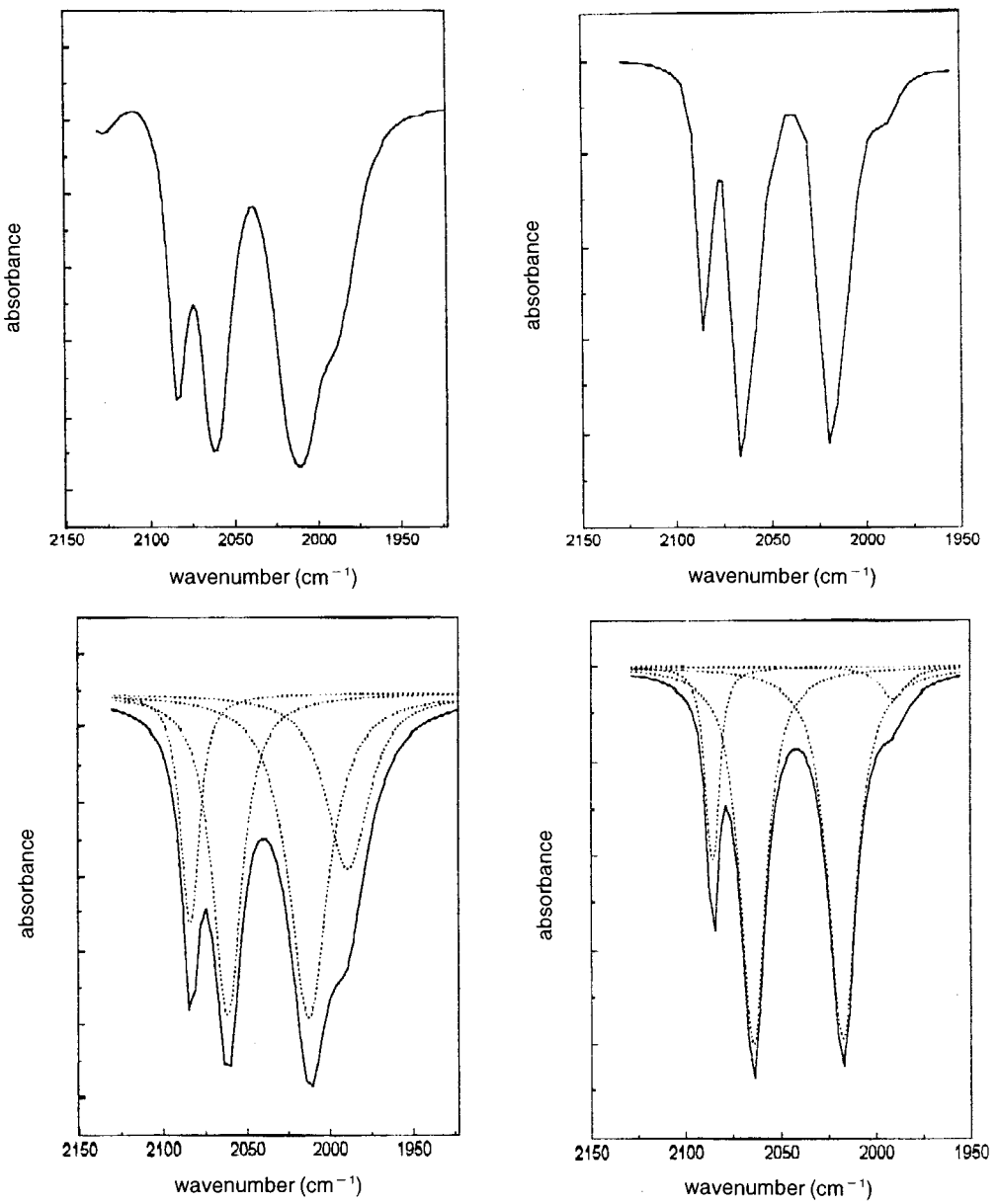

Fig. 2. Experimental IR spectrum in the carbonylic region of $[Rh_2(RiSS)(CO)_4]$ (**5**) (right) and $[Rh_2(XySS)(CO)_4]$ (**6**) (left) with its Lorentzian adjustment.

Table 2
Wavenumber (cm^{-1}) of the stretching carbonyl vibrations for $[Rh_2(\mu\text{–XySS})(CO)_4]$ (**6**) and $[Rh_2(\mu\text{-}(S(CH_2)_3S)(CO)_4]$

	ν_1	ν_2	ν_3	ν_4
$[Rh_2(\mu\text{-XySS})(CO)_4]$				
Experimental	2084	2062	2012	1989
Calculated	2102	2089	2041	2037
Difference	18	27	29	48
$[Rh_2(\mu\text{-}(S(CH_2)_3S)(CO)_4]$				
Experimental	2086	2065	2017	
Calculated	2104	2085	2042	
Difference	21	24	30	

It is generally accepted that the catalyst precursor $[Rh(acac)(CO)_2]$ evolves rapidily under hydroformylation conditions to the active species $[RhH(CO)_3]$ (not regioselective in these conditions). The results in entries 1 and 2 suggest a similar, though slower, evolution for the catalyst precursor **2**. In order to confirm this hypothesis, styrene was hydroformylated in the same conditions but with $[Rh(acac)(CO)_2]$ (**9**) as the precatalyst (entry 7). It is worth noting that the regioselectivity obtained in this experiment coincides with the value to which the results of entries 1 and 2 evolve. This indicates that complex **2** has little catalytic activity and that it transforms slowly and gradually to $[RhH(CO)_3]$. The fact that there are practically no enantiomeric excesses (less than 4%) further supports this hypothesis.

The catalyst precursor $[Rh_2(\mu\text{-RiSS})(cod)_2]$ (**1**) is more active at 30 bar and 75°C in the hydroformylation of styrene (entries 3 and 4). The regioselectivity again coincides with the result obtained with $[Rh(acac)(CO)_2]$ (entry 7). This system is also active at 10 and 20 bar (entries 5–6). The regioselectivities are again the same as the ones obtained with $[Rh(acac)(CO)_2]$ (**1**) in the same conditions (entries 8 and 9). These results and the practical absence of chiral induction supports the hypothesis formulated for the catalyst precursor **2**.

If the results obtained for catalyst precursors **1** and **2** are compared, it can be observed that **1** is more active, even at lower pressures, than **2**. According to our hypothesis, this means that, under hydroformylation conditions, **2** evolves more slowly than **1** to $[RhH(CO)_3]$, the major active species for this reaction.

The same reaction was carried out in the presence of triphenylphosphine and the conclusions were not very different (Table 5). The progressive formation of the mononuclear active species $[RhH(CO)_x(PPh_3)_{3-x}]$ under these conditions, as also described for $[Rh(acac)(CO)_2]/PPh_3$ system [30], is responsible for the catalytic activity observed. In this case the rupture of the dinuclear compound was faster than in the absence of triphenylphosphine.

These results agree with very recent high-pressure spectroscopic studies, carried out on rhodium complexes containing bridge dithiolate ligands and triphenylphosphine under hydroformylation conditions [31].

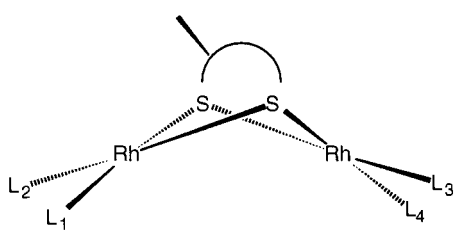

Isomer	L_1	L_2	L_3	L_4
cis	PPh_3	CO	CO	PPh_3
cis	CO	PPh_3	PPh_3	CO
trans	PPh_3	CO	PPh_3	CO
trans	CO	PPh_3	CO	PPh_3

Fig. 3. Possible geometric isomers for the stoichiometry $[Rh_2(\mu\text{-SS})(CO)_2(PPh_3)_2]$ where SS is a bridging asymmetric dithiolate ligand.

3. Conclusions

The epimer dithiolate ligands $RiSS^{2-}$ and $XySS^{2-}$ react with $[M(\mu\text{-OMe})(cod)]_2$ (M = Rh, Ir) to form the dinuclear dithiolate bridged complexes $[M_2(\mu\text{-RiSS})(cod)_2]$ and $[M_2(\mu\text{-XySS})(cod)_2]$. The rhodium complexes react with carbon monoxide to afford the corresponding $[Rh_2(\mu\text{-RiSS})(CO)_4]$ and $[Rh_2(\mu\text{-XySS})(CO)_4]$ complexes which in the presence of tryphenylphosphine evolve to $[Rh_2(\mu\text{-RiSS})(CO)_2(PPh_3)_2]$ and $[Rh_2(\mu\text{-XySS})(CO)_2(PPh_3)_2]$. All the complexes with $XySS^{2-}$ as bridging dithiolate can be present as two conformers. In the absence of steric hindrance, the most stable conformer is the one in which the oxygen of the furanose ring is above one of the rhodium atoms. DFT theoretical studies show the existence of a bond interaction between these two atoms which stabilizes the structure. Computed CO stretching frequencies for $[Rh_2(\mu\text{-XySS})(CO)_4]$ agree with the experimental values and confirm the dinuclearity of these complexes.

Between 5 and 30 bar *syn* gas, $[Rh_2(\mu\text{-RiSS})(cod)_2]$ and $[Rh_2(\mu\text{-XySS})(cod)_2]$ undergo a progressive rupture to mononuclear complexes that do not contain the dithiolate ligand and are the major active species in the hydroformylation of styrene.

Table 3
Strain energies for the possible isomers of the complex $[Rh_2(\mu\text{-XySS})(CO)_2(PPh_3)_2]$ (**8**)

Isomer	L_4	Relative conformation of the furanose ring	Strain energy (kcal mol^{-1})
cis	CO	a	130.6
trans	CO	a	131.6
cis	PPh_3	b	140.0
trans	PPh_3	b	141.2
cis	CO	b	138.4
trans	CO	b	139.6

4. Experimental

4.1. General comments

All syntheses were performed by standard Schlenk techniques under a nitrogen atmosphere. The complexes $[Rh(\mu\text{–OMe})(cod)]_2$ [32], $[Ir(\mu\text{–OMe})(cod)]_2$ [32b,33] $[Rh(acac)(CO)_2]$ [34], and the compounds 1,2-O-isopropylidene-α-D-xylofuranose [35] and 1,2-O-isopropylidene-α-D-ribofuranose [35,36] were prepared by previously described methods. Solvents were purified by standard procedures. All other reagents were used as commercially available.

Elemental analyses were performed on a Carlo Erba EA-1108 instrument. Infrared spectra (KBr pellet or solution) were obtained on a FT-IR MIDAC Prospect PRS instrument. IR Lorentz line shape analyses were performed with the Microcal Origin 4.1 Program. ^{1}H-, $^{13}C\{^1H\}$- and $^{31}P\{^1H\}$-NMR spectra were recorded on a Variant Gemini 300 MHz Spectrometer. Chemical shifts are relative to $SiMe_4$ (^{1}H and ^{13}C) as internal standard or H_3PO_4 (^{31}P) as external standard. All assignments in NMR spectra were determined by means of COSY and HETCOR spectra. EI Mass spectra were obtained on an HP 5989 A spectrometer. A VG-Autospect was used for FAB mass spectral analyses. The matrix was *m*-nitrobenzylalcohol. Gas chromatographic analyses were run on a Hewlett–Packard 5890A instrument (split/splitless injector, J&W Scientific, Ultra-2 25 m column, internal diameter 0.2 mm, film thickness 0.33 mm, carrier gas: 150 kPa He, F.I.D. detector) equipped with a Hewlett–Packard 3396 series II integrator. Enantiomeric excesses were measured after oxidation of the aldehydes to the corresponding carboxylic acids on a Hewlett–Packard 5890A gas chromatograph (split/splitless injector, J&W Scientific, FS-Cyclodex β-I/P 50 m column, internal diameter 0.2 mm, film thickness 0.33 mm, carrier gas: 100 kPa He, F.I.D. detector). Absolute configuration was determined by comparing the retention times with optically pure (*S*)-(+)-2-phenylpropionic and *R*-(−)-2-phenylpropionic acids. Optical rotations were measured at 25°C on a Perkin–Elmer 241 MC polarimeter. The specific rotations are given in deg cm^3 g^{-1} dm^{-1} units. Hydroformylation reactions were carried out in a home-made 100 cm^3 stainless steel autoclave.

4.2. Computational details

Density functional calculations were made with the ADF package [37]. For the correlation, the spin local density approximation for the electron gas exchange (Xα, $\alpha = 2/3$) was used with the Vosko–Wilk–Nusair parametrization [38]. Non-local corrections were applied self consistently, taking the gradient-corrected Becke's functional [39] for the exchange and Perdew's functional [40] for correlation, i.e. the so-called BP86 functional. A double-ζ + polarization Slater basis set was used to describe the valence electrons of C, O and S. For the Rh atoms, a frozen core composed of the 1s to 4sp shells was described with simple Slater functions. 5s and 4d electrons were described by triple-ζ Slater functions and 5p by a single orbital. The H atoms were described by a double-ζ Slater basis set. Quasi relativistic corrections were made using the Pauli formalism with corrected core potentials. The quasi relativistic frozen core shells were generated with the auxiliary program DIRAC [36].

The molecular mechanics calculations were carried out with the program CERIUS2 [41] developed by *Molecular Simulations* (MSI) and the force field UFF developed by Rappe et al. [42]. The electrostatic interactions were taken into account from atomic changes generated by the Qeq method [43].

Table 4
Hydroformylation of styrene with $[Rh_2(\mu\text{-SS})(cod)_2]$, SS = RiSS (**1**) or XySS (**2**) as precatalyst [a]

Entry	Precursor	*P* (bar)	*t* (h)	%Conv.	%2-PP
1	**2**	30	24	19	66
2	**2**	30	48	82	55
3	**1**	30	3	47	51
4	**1**	30	6	99	51
5	**1**	20	9	85	45
6	**1**	10	20	57	41
7	**9**	30	2	80	55
8	**9**	20	2.5	58	46
9	**9**	10	6	45	43

[a] Conditions: Substrate: Rh = 300. Solvent: tetrahydrofuran (7.5 cm^3). Precursor (0.05 mmol). $T = 75$°C. CO: $H_2 = 1.\%$ Conv. = conversion in aldehydes (chemoselectivity > 99%). 2-PP = 2-phenylpropanal.%2-PP = 100 × (2-PP)/(2-PP + 3-PP). 3-PP = 3-phenylpropanal. **9**: $[Rh(acac)(CO)_2]$.

Table 5
Hydroformylation of styrene with $[Rh_2(\mu\text{-SS})(cod)_2]$, SS = RiSS (**1**) or XySS (**2**) as precatalyst in the presence of PPh_3 [a]

Entry	Precursor	P (bar)	*t* (h)	%Conv.	%2-PP
1	**2**	5	20	13	63
2	**2**	30	2	100	89
3	**1**	5	7	76	61
4	**1**	30	1.5	100	89
5	**9**	5	1	98	61
6	**9**	30	0.6	96	89

[a] Conditions: Substrate: Rh = 200. PPh_3:Rh = 1. Solvent: tetrahydrofuran (7.5 cm^3). Precursor (0.05 mmol). $T = 75°C$. $CO:H_2 = 1$. % Conv. = conversion in aldehydes (chemoselectivity > 99%). 2-PP = 2-phenylpropanal. %2-PP = 100 × (2-PP)/(2-PP + 3-PP). 3-PP = 3-phenylpropanal. **9**: $[Rh(acac)(CO)_2]$.

Finally, the topological properties of the charge density were computed with a modified version of the AIMPAC package [44] and the Xaim software [45].

4.3. Synthesis of 1,2-O-isopropylidene-3,5-di-O-trifluoromethansulfonyl-α-D-xylofuranose (III) and 1,2-O-isopropylidene-3,5-di-O-trifluoromethansulfonyl-α-D-ribofuranose (IV)

Anhydrous pyridine (0.8 cm^3, 10 mmol) was added to a solution of 1,2-*O*-isopropylidene-α-D-xylofuranose or 1,2-*O*-isopropylidene-α-D-ribofuranose (0.7 g, 3.7 mmol) in 20 cm^3 methylene chloride. After 10 min, trifluoromethanesulfonic anhydride (1.5 cm^3, 8.9 mmol) was added dropwise at −20°C and the mixture was allowed to react at room temperature for 45 min after which the solvent was evaporated. The residue was purified by column chromatography (10:1 hexane–ethyl acetate) to give the ditriflate as a white solid.

4.3.1. Compound III

(0.9 g, 54%), $[\alpha]_D^{25}$ (*c* 1.25 in $CHCl_3$) = −19.2 (Found: C, 26.77; H, 2.68; S, 13.98. Calc. for $C_{10}H_{12}O_9S_2F_6$: C, 26.44; H, 2.66; S, 14.12%); $\delta_H(CDCl_3)$ 1.35 (3H, s, CH_3), 1.56 (3H, s, CH_3), 4.68 (3H, m, H-5, H-5′, H-4), 4.80 (1H, d, H-2, $J_{2-1} = 3.9$ Hz), 5.26 (1H, d, H-3, $J_{3-4} = 2.3$ Hz) and 6.06 (1H, d, H-1, $J_{1-2} = 3.9$ Hz); $\delta_C(CDCl_3)$ 26.1 (CH_3), 26.4 (CH_3), 70.5 (C-5), 75.6 (C-4), 83.0 (C-2), 86.8 (C-3), 104.8 (C-1), 113.8 (CMe_2), 118.3 (q, CF_3, $J_{C-F} = 305$ Hz) and 118.4 (q, CF_3, $J_{C-F} = 304$ Hz); *m*/*z*: 439 $[M^- CH_3]$.

4.3.2. Compound IV

(0.9 g 54%), $[\alpha]_D^{25}$ (*c* 1.25 in $CHCl_3$) = +54 (Found: C, 26.97; H, 2.96; S, 13.82. Calculated for $C_{10}H_{12}O_9S_2F_6$: C, 26.44; H, 2.66; S, 14.12%); $\delta_H(CDCl_3)$ 1.40 (3H, s, CH_3), 1.59 (3H, s, CH_3), 4.37 (1H, dt, H-4, $J_{4-5} = 2.2$ Hz, $J_{4-5'} = 2.2$ Hz, $J_{4-3} = 8.7$ Hz), 4.51 (1H, dd, H-5′, $J_{5'-5} = 11.9$ Hz, $J_{5'-4} = 2.2$ Hz), 4.73 (1H, dd, H-2, $J_{1-2} = 3.5$ Hz, $J_{2-3} = 4.1$ Hz), 4.78 (1H, dd, H-5, $J_{5-5'} = 11.9$ Hz, $J_{5-4} = 2.2$ Hz), 4.86 (1H, dd, H-3, $J_{3-2} = 4.1$ Hz, $J_{3-4} = 8.7$ Hz) and 5.80 (1H, d, H-1, $J_{1-2} = 3.5$ Hz); $\delta_C(CDCl_3)$ 26.5 (CH_3), 71.2 (C-5), 74.3 (C-4), 77.0 (C-2), 80.0 (C-3), 104.0 (C-1), 114.9 (CMe_2), 118.4 (q, CF_3, $J_{C-F} = 320$ Hz) and 118.5 (q, CF_3, $J_{C-F} = 318$ Hz).

4.4. Synthesis of 3,5-di-S-acetyl-1,2-O-isopropylidene-3,5-dithio-α-D-ribofuranose (V) and 3,5-di-S-acetyl-1,2-O-isopropylidene-3,5-dithio-α-D-xylofuranose (VI)

Potassium thioacetate (6.5 g, 59.9 mmol) was added to a acetonitrile solution (35 cm^3) of compound **III** or **IV** (2.0 g, 4.4 mmol) and the mixture was refluxed for 90 min. The solution was evaporated to dryness and the residue was extracted with CH_2Cl_2 (3 × 20 cm^3). The product, obtained after evaporating the dried solution ($MgSO_4$), was purified by column chromatography (5:1 hexane–ethyl acetate) to give a yellow solid.

4.4.1. Compound V

Yellow–orange product (310 mg, 23%), $[\alpha]_D^{25}$ (*c* 1.25 in $CHCl_3$) = +55.2 (Found: C, 47.32; H, 6.05; S, 21.36. Calc. for $C_{12}H_{18}O_5S_2$: C, 47.52; H, 5.94; S, 21.12%); $\delta_H(CDCl_3)$ 1.32 (3H, s, CH_3), 1.50 (3H, s, CH_3), 2.35 (3H, s, CH_3–CO), 2.39 (3H, s, CH_3–CO), 3.10 (1H, dd, H–5′, $J_{5'-5} = 14.3$ Hz, $J_{5'-4} = 6.3$ Hz), 3.32 (1H, dd, H-5, $J_{5-5'} = 14.3$ Hz, $J_{5-4} = 4.1$ Hz), 3.74 (1H, dd, H-3, $J_{3-4} = 10.3$ Hz, $J_{3-2} = 4.1$ Hz), 4.12 (1H, ddd, H-4, $J_{4-3} = 10.3$ Hz, $J_{4-5'} = 6.3$ Hz, $J_{4-5} = 4.1$ Hz), 4.70 (1H, dd, H-2, $J_{2-1} = 3.9$ Hz, $J_{2-3} = 4.1$ Hz) and 5.84 (1H, d, H-1, $J_{1-2} = 3.9$ Hz); $\delta_C(CDCl_3)$ 26.2 (CH_3), 26.5 (CH_3), 29.9 (C-5), 33.0 (CH_3–CO), 47.5 (C-3), 78.7 (C-4), 80.9 (C-2), 104.4 (C-1), 112.3 (CMe_2), 194.0 (CO) and 194.7 (CO); *m*/*z* 291 [M–CH_3], 263 [M–$COCH_3$].

4.4.2. Compound VI

Pale yellow product (935 mg, 70%), $[\alpha]_D^{25}$ (*c* 1.25 in $CHCl_3$) = −34 (Found: C, 26.97; H, 2.96; S, 13.82. Calc. for $C_{10}H_{12}O_9S_2F_6$: C, 26.44; H, 2.66; S, 14.12%); $\delta_H(CDCl_3)$ 1.30 (3H, s,CH_3), 1.52 (3H, s, CH_3), 2.38(3H, s, CH_3–CO), 2.41 (3H, s, CH_3–CO), 3.04 (1H, dd, H-5′, $J_{5'-5} = 13.7$ Hz, $J_{5'-4} = 6.4$ Hz), 3.21 (1H, dd, H-5, $J_{5-5'} = 13.7$ Hz, $J_{5-4} = 7.7$ Hz), 4.13 (1H, d, H-3, $J_{3-4} = 3.7$ Hz), 4.48 (1H, ddd, H-4, $J_{4-5'} = 6.4$ Hz, $J_{4-5} = 7.7$ Hz, $J_{4-3} = 3.7$ Hz), 4.58 (1H, d, H-2, $J_{2-1} = 3.7$ Hz) and 5.80 (1H, d, H-1, $J_{1-2} = 3.7$ Hz); $\delta_C(CDCl_3)$ 26.2 (CH_3), 26.5 (CH_3), 29.1 (C-5), 30.5 (CH_3–CO), 31.0 (CH_3–CO), 51.0 (C-3), 77.0 (C-4), 86.3 (C-2), 104.5 (C-1), 112.1 (CMe_2), 192.9 (CO) and 194.6 (CO); *m*/*z* 263 [M − $COCH_3$], 220 [M − 2$COCH_3$].

4.5. Synthesis of 1,2-O-isopropylidene-3,5-dithiol-α-D-ribofuranose (RiSSH2) and 1,2-O-isopropylidene-3,5-dithiol-α-D-xylofuranose ($XySSH_2$)

Compound **V** or **VI** (0.05 g, 0.16 mmol) was added to a suspension of 15.0 mg of the ion-exchange resin IRA 420 (Fluka) in 5 cm^3 methanol and the mixture was allowed to react for 24 h. After filtration and evaporation of the solvent the product was obtained as a white solid.

4.5.1. RiSSH2

(29.5 mg, 80%), $[\alpha]_D^{25}$ (c 1.25, $CHCl_3$) = +100.8 (Found: C, 42.92; H, 6.35; S, 28.15. Calc. for $C_8H_{14}O_3S_2$: C, 43.23; H, 6.35; S, 28.85%); $\delta_H(CDCl_3)$ 1.36 (3H, s, CH_3), 1.52 (3H, s, CH_3), 1.60 (1H, dd, HS-C-5, $J_{SH-5'}$ = 11.7 Hz, J_{SH-5} = 4.7 Hz), 1.79 (1H, d, HS–C-3, J_{SH-3} = 13.1 Hz), 2.74 (1H, ddd, H-+5′, $J_{5'-5}$ = 14.0 Hz, $J_{5'-SH}$ = 11.7 Hz, $J_{5'-4}$ = 5.1 Hz), 3.07 (2H, m, H–5, H-3), 3.94 (1H, m, H-4), 4.63 (1H, dd, H-2, J_{2-3} = 4.0 Hz, J_{2-1} = 3.9 Hz) and 5.82 (1H, d, H-1, J_{1-2} = 3.9 Hz);.$\delta_C(CDCl_3)$ 25.1 (C-5), 26.4 (CH_3), 26.5 (CH_3), 42.3 (C-3), 81.3 (C-2), 82.8 (C-4), 104.0 (C-1) and 112.0 (CMe_2); m/z 220 [$M^{+\bullet}$–2H], 189 [$M^{+\bullet}$–SH].

4.5.2. $XySSH_2$

(35.0 mg, 95%), $[\alpha]_D^{25}$ (c 1.25 in $CHCl_3$) = +289 (Found: C, 43.92; H, 5.71; S, 27.23. Calc. for $C_8H_{14}O_3S_2$: C, 43.23; H, 6.35; S, 28.85%); $\delta_H(CDCl_3)$ 1.35 (3H, s, CH_3), 1.54 (3H, s, CH_3), 2.99 (1H, dd, H-5′, $J_{5'-5}$ = 12.7 Hz, $J_{5'-4}$ = 3.0 Hz), 3.41 (1H, d, H-5, $J_{5-5'}$ = 12.7 Hz), 4.11 (1H, d, H-3, J_{3-4} = 5.4 Hz), 4.76 (1H, d, H-2, J_{2-1} = 3.9 Hz), 5.48 (1H, m, H-4) and 5.93 (1H, d, H-1, J_{1-2} = 3.9 Hz); $\delta_C(CDCl_3)$ 26.9 (CH_3), 27.5 (CH_3), 49.3 (C-5), 61.1 (C-3), 88.0 (C-2), 88.2 (C-4), 106.5 (C-1) and 112.7 (CMe_2); m/z 220 [M − 2H], 189 [M–SH].

4.6. Synthesis of [Rh_2(μ-RiSS)(cod)$_2$] (**1**) and [Rh_2(μ-XySS)(cod)$_2$] (**2**)

Bisthioacetate **V** or **VI** (0.1 mmol, 30.8 mg) and sodium methoxide (0.1 mmol, 5.5 mg) were added to a solution of [Rh(μ-OMe)(cod)]$_2$ (0.1 mmol, 44.4 mg) in 2 cm^3 of methylene chloride and the mixture was allowed to react for 6 h. After precipitation with methanol, the red product was filtered, washed with cold methanol and vacuum dried.

4.6.1. [Rh_2(μ-RiSS)(cod)$_2$] (**1**)

(39 mg, 65%) (Found: C, 45.15; H, 5.65; S, 9.98. Calc. for $Rh_2C_{24}H_{36}O_3S_2$: C, 44.87; H, 5.65; S, 9.98%); $\delta_H(CD_2Cl_2)$ 1.30 (3H, s, CH_3), 1.66 (3H, s, CH_3), 1.95 (4H, m, CH_2 COD), 2.12 (4H, m, CH_2 COD), 2.33 (4H, m, CH_2 COD), 2.49 (5H, m, CH_2 COD, H-5'), 2.64 (1H, m, H-5), 4.16 (5H, m, CH COD, H-4), 4.39 (1H, dd, H-2, J_{2-1} = 4.1 Hz, J_{2-3} = 3.9 Hz), 4.52 (3H, m, CH COD, H-3), 4.76 (2H, m, CH COD) and 5.55 (1H, d, H-1, J_{1-2} = 4.1 Hz); $\delta_C(CD_2Cl_2)$ 26.5 (CH_3), 26.6 (CH_3), 31.6 (CH_2 COD), 31.7 (CH_2 COD), 31.9 (CH_2 COD), 32.0 (CH_2 COD), 32.1 (CH_2 COD), 32.2 (CH_2 COD), 34.6 (C-5), 51.8 (C-3), 80.5 (d, CH COD, J_{C-Rh} = 10.7 Hz), 81.8 (d, CH COD, J_{C-Rh} = 10.3 Hz), 81.9 (d, CH COD, J_{C-Rh} = 11.8 Hz), 82.1 (d, CH COD, J_{C-Rh} = 10.6 Hz), 82.2 (d, CH COD, J_{C-Rh} = 12.5 Hz), 82.4 (C-2), 82.6 (d, CH COD, J_{C-Rh} = 10.6 Hz), 83.7 (d, CH COD, J_{C-Rh} = 10.3 Hz), 83.9 (d, CH COD, J_{C-Rh} = 11.2 Hz), 87.0 (C-4), 104.6 (C-1) and 111.9 (CMe_2); m/z 642 [M^+].

4.6.2. [Rh_2(μ-XySS)(cod)$_2$] (**2**)

(36 mg, 60%) (Found: C, 44.74; H, 5.72; S, 9.87. Calc. for $Rh_2C_{24}H_{36}O_3S_2$: C, 44.87; H, 5.65; S, 9.98%); $\delta_H(CD_2Cl_2)$ 1.27 (3H, s, CH_3), 1.39 (3H, s, CH_3), 1.88 (4H, m, CH_2 COD), 2.11 (4H, m, CH_2 COD), 2.29 (4H, m, CH_2 COD), 2.50 (4H, m, CH_2 COD), 2.62 (1H, dd, H-5′, $J_{5'-5}$ = 12.7 Hz, $J_{5'-4}$ = 3.4 Hz), 2.86 (2H, m, H-5, H-3), 3.91 (1H, m, CH COD), 3.97 (1H, m, CH COD), 4.15(3H, m, CH COD, H-4), 4.38 (1H, d, H-2, J_{2-1} = 4.2 Hz), 4.42 (2H, m, CH COD), 4.58 (2H, m, CH COD) and 6.34 (1H, d, H-1, J_{1-2} = 4.2 Hz); $\delta_C(CD_2Cl_2)$ 26.3 (CH_3), 26.8 (CH_3), 30.2 (C-5), 31.3 (CH_2 COD), 31.5 (CH_2 COD), 31.9 (CH_2 COD), 32.0 (CH_2 COD), 32.6 (CH_2 COD), 34.0 (CH_2 COD), 49.7 (C-3), 77.8 (C-2), 79.7 (d, CH COD, J_{C-Rh} = 9.4 Hz), 80.2 (d, CH COD, J_{C-Rh} = 9.4 Hz), 80.9 (d, CH COD, J_{C-Rh} = 9.5 Hz), 81.6 (d, CH COD, J_{C-Rh} = 10.0 Hz), 81.9 (d, CH COD, J_{C-Rh} = 9.5 Hz), 82.4 (d, CH COD, J_{C-Rh} = 9.5 Hz), 83.1 (d, CH COD, J_{C-Rh} = 9.5 Hz), 90.0 (C-4), 105.1 (C-1) and 111.7 (CMe_2); m/z 642 [M^+].

4.7. Synthesis of [Ir_2(μ-RiSS)(cod)$_2$] (**3**) and [Ir_2(μ-XySS)(cod)$_2$] (**4**)

Bisthioacetate **V** or **VI** (0.07 mmol, 21.0 mg) and sodium methoxide (0.07 mmol, 4.0 mg) were added to a solution of [Ir(μ-OMe)(cod)]$_2$ (0.06 mmol, 40.0 mg) in 2 cm^3 of methylene chloride and the mixture was allowed to react for 2 h. The red solution was filtered over celite in order to remove the sodium methoxide, and the product was obtained after precipitation with cold petroleum ether.

4.7.1. [Ir_2(μ-RiSS)(cod)$_2$] (**3**)

(26 mg, 53% yield) (Found: C, 33.34; H, 4.22; S, 7.13. Calc. for $Ir_2C_{24}H_{36}O_3S_2 + CH_2Cl_2$: C, 33.14; H, 4.23; S, 7.07%); m/z 819 [M^+ − 2H].

4.7.2. [Ir_2(μ-XySS)(cod)$_2$] (**4**)

(10 mg, 21% yield) (Found: C, 34.66; H, 4.45; S, 6.95. Calc. for $Ir_2C_{24}H_{36}O_3S_2$: C, 35.11; H, 4.42; S, 7.81%); m/z 820 [M^+ − H].

4.8. Synthesis of [Rh_2(μ-RiSS)$(CO)_4$] (5) and [Rh_2(μ-XySS)$(CO)_4$] (6)

Carbon monoxide was bubbled for 15 min through a solution of [Rh_2(μ-RiSS)$(cod)_2$] or [Rh_2(μ-XySS)$(cod)_2$] (40 mg, 0.06 mmol) in 5 cm^3 deuterated dichloromethane. The red solution turned green.

4.8.1. [Rh_2(μ-RiSS)$(CO)_4$] (5)

ν_{max}/cm^{-1} (CO) 2086, 2065, 2017 and 1990 (CH_2Cl_2); $\delta_H(CD_2Cl_2)$ 1.32 (3H, s, CH_3), 1.62 (3H, s, CH_3), 2.36 (8H, m, CH_2 free COD), 2.44 (1H, dd, H-5′, $J_{5'-4}=10.7$ Hz, $J_{5'-5}=10.1$ Hz), 2.89 (1H, dd, H-5, $J_{5-5'}=10.1$ Hz, $J_{5-4}=4.4$ Hz), 3.00 (1H, dd, H-3, $J_{3-4}=11.8$, $J_{3-2}=3.3$ Hz), 4.09 (1H, m, H-4), 4.58 (1H, dd, H-2, $J_{2-1}=3.6$ Hz, $J_{2-3}=3.3$ Hz), 5.54 (4H, m, CH free COD) and 5.66 (1H, d, H-1, $J_{1-2}=3.6$ Hz); $\delta_C(CD_2Cl_2)$ 25.3 (CH_3), 25.6 (CH_3), 27.3 (CH_2 free COD), 33.5 (C-5), 50.4 (C-3), 80.2 (C-2), 85.0 (C-4), 104.1 (C-1), 111.6 (CMe_2), 127.9 (CH free COD) and 183.6 (d, CO, $J_{Rh-CO}=72$ Hz).

4.8.2. [Rh_2(μ-XySS)$(CO)_4$] (6)

ν_{max}/cm^{-1} (CO) 2084, 2062, 2013 and 1989 (CH_2Cl_2); $\delta_H(CD_2Cl_2)$ 1.29 (3H, s, CH_3), 1.43 (3H, s, CH_3), 2.34 (8H, m, CH_2 free COD), 3.00 (1H, dd, H-5′, $J_{5'-4}=2.9$ Hz, $J_{5'-5}=14.6$ Hz), 3.15 (1H, dd, H-5, $J_{5-5'}=14.6$ Hz, $J_{5-4}=2.2$ Hz), 3.30 (1H, d, H-3, $J_{3-4}=2.9$ Hz), 4.43 (1H, td, H-4, $J_{4-3}=J_{4-5'}=2.9$ Hz, $J_{4-5}=2.2$ Hz), 4.60 (1H, d, H-2, $J_{2-1}=3.7$ Hz), 5.54 (4H, m, CH free COD) and 6.16 (1H, d, H-1, $J_{1-2}=3.7$ Hz); $\delta_C(CD_2Cl_2)$ 26.2 (CH_3), 26.3 (CH_3), 28.3 (CH_2 free COD), 31.0 (C-5), 49.7 (C-3), 76.1 (C-2), 88.8 (C-4), 104.5 (C-1), 111.9 (CMe_2), 128.8 (CH free COD) and 182.6 (d, CO, $J_{Rh-CO}=70$ Hz).

4.9. Synthesis of [Rh_2(μ-RiSS)$(CO)_2(PPh_3)_2$] (7) and [Rh_2(μ–XySS)$(CO)_2(PPh_3)_2$] (8)

Carbon monoxide was bubbled through a solution of [Rh_2(μ-RiSS)$(cod)_2$] or [Rh_2(μ-XySS)$(cod)_2$] (40 mg, 0.06 mmol) in the minimum amount of dichloromethane. The red solution turned green. After 15 min, triphenylphosphine (38.9 mg, 0.12 mmol) was added and the green solution turned orange. The mixture was allowed to react for 20 min at room temperature. An orange product was obtained by precipitation with hexane.

4.9.1. [Rh_2(μ-RiSS)$(CO)_2(PPh_3)_2$] (7)

(32 mg, 52%) (Found: C, 55.38; H,4.32; S, 5.98. Calc. for $Rh_2C_{46}H_{42}O_5S_2P_2$: C, 54.88; H, 4.20; S, 6.37%); ν_{max}/cm^{-1} (CO) 2021, 1992 and 1969 cm^{-1} (CH_2Cl_2); 1967 (KBr); m/z 1006 [M^+].

4.9.2. Minor isomers

$\delta_H(CD_2Cl_2)$ 1.54 (3H, s, CH_3), 1.61 (3H, s, CH_3), 3.01 (2H, m, H-5 i H-5′), 3.27 (1H, m, H-3), 4.78 (2H, m, H-2 i H-4), 5.81 (1H, d, H-1, $J_{1-2}=3.8$ Hz) and 7.2–8.0 (CH, Ph); $\delta_P(CD_2Cl_2)$ 39.4 (1P, d, $J_{P-Rh}=11.9$ Hz), 40.1 (1P, d, $J_{P-Rh}=10.7$ Hz), 40.7 (1P, d, $J_{P-Rh}=12.3$ Hz) and 41.2 (1P, m).

4.9.3. Major isomers

$\delta_H(CD_2Cl_2)$ 1.49 (3H, s, CH_3), 1.78 (3H, s, CH_3), 2.50 (2H, m, H-5 i H-5′), 2.72 (1H, m, H-3), 4.39 (2H, m, H-2 i H-4), 5.79 (1H, d, H-1, $J_{1-2}=3.8$ Hz) and 7.2–8.0 and (CH, Ph) $\delta_P(CD_2Cl_2)$ 39.9 (1P, d, $J_{P-Rh}=14.9$ Hz), 41.2 (2P, m) and 42.6 (1P, d, $J_{P-Rh}=14.8$ Hz).

4.9.4. [Rh_2(μ–XySS)$(CO)_2(PPh_3)_2$] (8)

(35 mg, 57%) (Found: C, 55.38; H, 4.32; S, 5.98. Calc. for $Rh_2C_{46}H_{42}O_5S_2P_2$: C, 54.88; H, 4.20; S, 6.37%); ν_{max}/cm^{-1} (CO) 2020, 1991 and 1966 (CH_2Cl_2); 1965 (KBr); m/z 1006 [M^+].

4.9.5. Minor isomers

$\delta_H(CD_2Cl_2)$1.05 (3H, s, CH_3), 1.28 (3H, s, CH_3), 2.61 (2H, m, H-5 i H-5′), 3.18 (1H, m, H-3), 3.55 (1H, d, H-2, $J_{2-1}=3.3$ Hz), 4.30 (1H, m, H-4), 4.89 (1H, d, H-1, $J_{1-2}=3.3$ Hz) and 7.2–8.0 (CH, Ph); $\delta_P(CD_2Cl_2)$ 39.8 (d, 1P, $J_{P-Rh}=15.6$ Hz), 40.3 (d, 1P, $J_{P-Rh}=13.5$ Hz), 41.1 (d, 1P, $J_{P-Rh}=11.9$ Hz) and 41.6 (d, 1P, $J_{P-Rh}=13.9$ Hz).

4.9.6. Major isomers

$\delta_H(CD_2Cl_2)$ 1.21 (3H, s, CH_3), 1.43 (3H, s, CH_3), 2.89 (2H, m, H-5 i H-5′), 3.18 (1H, m, H-3), 4.45 (1H, d, H-2, $J_{2-1}=3.6$ Hz), 4.53 (1H, m, H-4), 6.29 (1H, d, H-1, $J_{1-2}=3.6$ Hz) and 7.2–8.0 (CH, Ph); $\delta_P(CD_2Cl_2)$ 39.6 (d, 1P, $J_{P-Rh}=14.2$ Hz), 40.8 (d, 1P, $J_{P-Rh}=11.9$ Hz), 42.0 (d, 1P, $J_{P-Rh}=12.3$ Hz) and 42.3 (d, 1P, $J_{P-Rh}=13.9$ Hz).

4.10. Hydroformylation of styrene

The autoclave was purged three times with CO. In the case of hydroformylations in the absence of triphenylphosphine, a THF solution (7.5 cm^3) of [Rh_2(μ-RiSS)$(cod)_2$] or [Rh_2(μ-XySS)$(cod)_2$] (0.025 mmol) and styrene (15 mmol) was introduced. When the hydroformylations were run in the presence of triphenylphosphine, the solution was formed from [Rh_2(μ-RiSS)$(cod)_2$] or [Rh_2(μ-XySS)$(cod)_2$] (0.025 mmol), triphenylphosphine (0.125 mmol) and styrene (10 mmol) in THF (7.5 cm^3). After pressurizing to the desired pressure with *syn* gas and heating the autoclave to the reaction temperature, the reaction mixture was stirred. During the reaction several samples were taken from the autoclave. After the desired reaction time, the autoclave was cooled to room temperature and depressurized. The reaction mixture was analysed by gas chromatography.

In order to determine the enantioselective excess, the aldehydes obtained from the hydroformylation were oxidized to carboxylic acids. A small portion of the hydroformylation reaction mixture (2 cm^3) was added to the solution formed with 10 cm^3 of a potassium permanganate 1 M solution and 10 cm^3 of a 1.25 M potassium dihydrogenphosphate solution. After 1 h with agitation, 5 cm^3 of a saturated solution of sodium sulfite was added and then diluted hydrochloric acid until the brown precipitate of manganese (IV) oxide disappeared. The acids formed were extracted with diethyl ether (3×10 cm^3) and the organic phase was concentrated to dryness. 10 cm^3 of a 2 M solution of sodium hydroxide were added. After washing the solution with diethyl ether, 10 cm^3 of concentrated hydrochloric acid were added and the product extracted with diethyl ether (3×10 cm^3). The carboxylic acids were obtained after washing the etheric phase with water, drying it with magnesium sulfate and evaporating it to dryness.

Acknowledgements

We thank the Spanish Ministerio de Educación y Cultura and the Generalitat de Catalunya (CIRIT) for financial support (QFN-95-4725-C03-2; PB95-0639-C02-02; CICYT-CIRIT) and the Generalitat de Catalunya (CIRIT) for awarding a research grant (to O.P.). We are also very much indebted to Prof. Sergio Castillón for his very useful discussions and suggestions on this work and to Ms Cinta Pujol for the IR Lorentz line shape analyses.

References

[1] (a) J.D. Morrison (Ed.), Asymmetric Synthesis, vol. 5, Academic Press: NY, 1985. (b) P.A. Chaloner, Handbook of Coordination Catalysis in Organic Chemistry, Butterworths, London, 1986. (c) H. Brunner, Topics in Stereochem. 18 (1988) 129. (d) H. Brunner, Synthesis (1988) 645. (e) M. Noyori, M. Kitamura, Modern Synthetic Methods 5 (1989) 155. (f) I. Ojima, M. Clos, C. Bastos, Tetrahedron 45 (1989) 6901. (g) R. Noyori, H. Takaya, Acc. Chem. Res. 23 (1990) 345. (h) M. Sasaya, Y. Ito, Chem. Rev. 92 (1992) 857. (i) H.U. Blaser, Chem. Rev. 92 (1992) 935. (j) I. Ojima (Ed.), Catalytic Asymmetric Synthesis, VCH, Weinheim, 1993. (k) R. Noyori, Asymmetric Catalysis in Organic Synthesis, Wiley, New York, 1994.

[2] (a) M. Bols, Carbohydrate Building Blocks, Wiley, New York, 1996. (b) W.A. Nugent, T.V. RajanBabu, M.J. Burk, Science 259 (1993) 479.

[3] (a) J.D. Morrison, J.W. Scott, Asymmetric Synthesis, vol. 14, Academic Press, San Diego, 1984. (b) J.S. Penne, Chiral Auxiliaries and Ligands in Asymmetric Synthesis, Wiley, New York, 1995.

[4] H. Brunner, W. Zettlmeier, Handbook of Enantioselective Catalysis, VCH, Weinheim, 1993.

[5] (a) M. Sawamura, K. Kitayama, Y. Ito, Tetrahedron Asymm. 4 (1993) 1829. (b) J.E. Babiarz, S.D. Pastor, Phosphorus, Sulfur and Silicon 91 (1994) 263. (c) G.J.H. Buisman, M.E. Martin, E.J. Voss, A. Klootwijk, P.C.J. Kamer, P.W.N.M. van Leeuwen, Tetrahedron: Asymmetry 6 (1995) 719. (d) J.-C. Shi, X.-Y. Huang, D.-X. Wu, Q.-T. Liu, B.-S. Kang, Inorg. Chem. 35 (1996) 2742. (e) M. Beller, J.G.E. Krauter, A. Zapf, Angew. Chem. Int. Ed. Engl. 36 (1997) 772. (f) M.T. Reetz, S.R. Waldvogel, Angew. Chem. Int. Ed. Engl. 36 (1997) 865.

[6] (a) DuPont, A.L. Casalnuovo, T.V. RajanBabu, US Patent, 5 484 902 (16 Jan. 1966). (b) T.V. Rajanbabu, A.L. Casalnuovo, Pure and Appl. Chem. 66 (1994) 1535. (c) A.L. Casalnuovo, T.V. RajanBabu, T.A. Ayers, T.H. Warren, J. Am. Chem. Soc. 116 (1994) 9869. (d) T.V. RajanBabu, A.L. Casalnuovo, J. Am. Chem. Soc. 118 (1996) 6325.

[7] (a) D. Lafont, D. Sinou, G. Descotes, J. Organomet. Chem. 169 (1979) 87. (b) S. Saito, Y. Nakamura, Y. Morita, Chem. Pharm. Bull. 33 (1985) 5284. (c) R. Selke, H. Pracejus J. Mol. Catal. 37 (1986) 213. (d) R. Selke, J. Organomet. Chem. 370 (1989) 241. (e) R. Selke, J. Organomet. Chem. 370 (1989) 249. (f) R. Selke, C. Facklam, H. Foken, D. Heller, Tetrahedron: Asymmetry 4 (1993) 369. (g) T.V. RajanBabu, T.A. Ayers, A.L. Casalnuovo, J. Am. Chem. Soc. 116 (1994) 4101. (h) A. Kumar, G. Oehme, J.P. Roque, M. Schwarze, R. Selke, Angew. Chem 106 (1994) 2272; Angew. Chem. Int. Ed. Engl. 33 (1994) 2197. (i) T.V. RajanBabu, T.A. Ayers, G.A. Halliday, K.K. You, J.C. Calabrese, J. Org. Chem. 62 (1997) 6012.

[8] A. Iida, M. Yamashita, Bull. Chem. Soc, Jpn. 61 (1988) 2365.

[9] T.V. Rajanbabu, T.A. Ayers, Tetrahedron Lett. 35 (1994) 4295.

[10] W. Vocke, R. Hänel, F. -U. Flöther, Chem. Tech. (Leipzig) 39 (1987) 123.

[11] M. Spescha, Helv. Chim. Acta 76 (1993) 1833.

[12] C. Li, B. Bernet, A. Vasella, E.A. Broger, A. Meili, Carbohydr. Res. 216 (1991) 149.

[13] (a) P. Barbaro, A. Currao, J. Herrmann, R. Nesper, P.S. Pregosin, R. Salzmann, Organometallics 15 (1996) 1879. (b) A. Albinati, P.S. Pregosin, K. Wick, Organometallics 15 (1996) 2419. (c) A. Albinati, J. Eckert, P.S. Pregosin, H. Rüegger, R. Salzmann, C. Stössen, Organometallics 16 (1997) 579.

[14] A. Borwitzky, T. Schareina, E. Paetzold, G. Oehme, Phosphorus Sulfur and Silicon and the related elements 114 (1996) 115.

[15] (a) P. Kalck, J.M. Frances, P.M. Pfister, T.G. Southern, A. Thorez, J. Chem. Soc. Chem. Commun. (1983) 510. (b) J.C. Bayón, J. Real, C. Claver, A. Polo, A. Ruiz, J. Chem. Soc. Chem. Commun. (1989) 1056. (c) S. Gladiali, J.C. Bayón, C. Claver, Tetrahedron: Asymmetry 8 (1995) 1453. (d) M. Diéguez, A. Orejón, A.M. Masdeu-Bultó, R. Echarri, S. Castillón, C. Claver, A. Ruiz, J. Chem. Soc. Dalton Trans. (1997) 4611. (e) M. Diéguez, A. Ruiz, C. Claver, M.M. Pereira, A.M. d'A. Rocha Gonsalves, J. Chem. Soc., Dalton Trans. (1988) 3517.

[16] F. Fache, P. Gamez, F. Nour, M. Lemaire, J. Mol. Catal. 85 (1993) 131.

[17] (a) C. Claver, S. Castillón, N. Ruiz, G. Delogu, D. Fabbri, S. Gladiali, J. Chem. Soc. Chem. Commun. (1993) 1833. (b) A.M. Masdéu, A. Orejón, A. Ruiz, S.Castillón, C. Claver, J. Mol. Catal. 94 (1994) 149. (c) A. Aaliti, A.M. Masdéu, A. Ruiz, C. Claver, J. Organomet. Chem. 489 (1995) 101. (d) A. Castellanos-Páez, S. Castillón, C. Claver, J. Organomet. Chem. 539 (1997) 1. (e) N. Ruiz, A. Aaliti, J. Forniés-Cámer, A. Ruiz, C. Claver, C.J. Cardin, D. Fabbri, S. Gladiali, J. Organomet. Chem. 545–546 (1997) 79. (f) J. Forniés-Cámer, A. Aaliti, N. Ruiz, A.M. Masdéu-Bultó, C. Claver, C.J. Cardin, J. Organomet. Chem. 539 (1997) 199.

[18] D.M.C. Hull, P.F. Ochard, L.N. Owen, J. Chem. Soc. Perkin Trans. I 10 (1977) 1234.

[19] (a) A.M. Masdeu, A. Ruiz, S. Castillón, C. Claver, P.B. Hitchcock, P. Chaloner, C. Bo, J.M. Poblet, P. Sarasa, J. Chem. Soc. Dalton Trans. (1993) 2689. (b) N. Ruiz, S. Castillón, A. Ruiz, C. Claver, A. Aaliti, A. Alvarez-Larena, F. Piniella, G. Germain, J. Chem. Soc. Dalton Trans. (1996) 969.

[20] R.V. Parish, NMR, NQR, EPR, Mössbauer Spectroscopy in Inorganic Chemistry, Ellis Horwood, Chichester, UK, 1990.
[21] (a) C. Claver, A.M. Masdéu, N. Ruiz, C. Foces-Foces, F.H. Cano, M.C. Apreda, L.A. Oro, J. García-Alejandre, H. Torrens, J. Organomet. Chem. 398 (1990) 177. (b) J. Pursiainen, T. Teppana, S. Rossi, A. Pakkanen, Acta Chem. Scan. 47 (1993) 416. (c) J.J. Bonnet, D. de Montauzon, R. Poilblanc, J. Galy, Acta Crystallogr. B35 (1979) 832.
[22] (a) E. Folga, T. Ziegler, J. Am. Chem. Soc. 115 (1995) 5169. (b) J. Li, G. Schreckenbach, T. Ziegler, Inorg. Chem. 34 (1995) 3245. (c) R.G. Parr, W. Yang, Density-functional Theory of Atoms, Molecules, Oxford University Press, New York, 1989. (d) E.S. Kryachko, E.V. Ludena, Density Functional Theory of Many Electron Systems, Kluwer Press, Dordrecht, 1990.
[23] A. Elduque, L.A. Oro, M.T. Pinillos, A. Tiripicchio, F. Ugozzoli, J. Chem. Soc. Dalton Trans. 3 (1994) 385.
[24] M. Cowie, J.T. Magne, A.R. Sanger, J. Am. Chem. Soc. 100 (1978) 3628.
[25] (a) R.F.W. Bader, Atoms in Molecules. A Quantum Theory; Clarendon Press, Oxford, 1990. (b) R.F.W. Bader, Chem. Rev. 91 (1992) 893.
[26] P. Kalck, R. Poilblanc, Inorg. Chem. 14 (1975) 2779.
[27] (a) A.W. Ehler, Y. Ruiz-Morales, E.I. Baerends, T. Ziegler, Inorg. Chem. 36 (1997) 5031. (b) R.K. Szilagyi and G. Frenking, Organometallics 16 (1997) 4807. (c) V. James, W. Thiel, Organometallics 17 (1998) 353.
[28] (a) J.J. Bonnet, J.P. Kalck, A. Maisonnat, R. Poilblanc, Inorg. Chem. 14 (1975) 743. (b) J.J. Bonnet, J.P. Kalck, R. Poilblanc, Inorg. Chem. 16 (1977) 1514.
[29] A. Polo, C. Claver, S. Castillón, A. Ruiz, J.C. Bayón, J. Real, C. Mealli, D. Masi, Organometallics 11 (1992) 3525.
[30] A.M. Trzeciak, J.J. Ziolkowski, S. Aygen, R. van Eldik, J. Mol. Catal. 34 (1986) 337.
[31] M. Diéguez, C. Claver, A.M. Masdéu-Bultó, A. Ruiz, P.W.N.M. van Leeuwen, G.C. Schoemaker, Organometallics 18 (1999) 2107.
[32] (a) G. Giordano, R.H. Crabtree, Inorg. Synth. 19 (1979) 218. (b) R. Usón, L.A. Oro, J.A. Cabeza, Inorg. Synth. 23 (1985) 126.
[33] (a) G. Winkhaus, H. Singer, Chem. Ber. 99 (1966) 3610. (b) J. Chatt, J.M. Davidson, J. Chem. Soc. (1965) 843.
[34] (a) J. Gallay, D. de Montouzon, R. Poilblanc, J. Organomet. Chem. 38 (1972) 179. (b) F. Bonati, G. Wilkinson, J. Chem. Soc. (1964) 3156.
[35] (a) K.P.R. Kartha, Tetrahedron Let. 27 (1986) 3415. (b) A.I. Vogel, Vogel's Textbook of Practical Organic Chemistry, 5th edition, Longman, NY, 1994.
[36] (a) P.A. Levene, A.L. Raymond, J. Biol. Chem. 102 (1933) 317. (b) D.H. Hollenberg, R.S. Klein, J.J. Fox, Carbohydr. Res. 67 (1978) 491. (c) G. Ritzmann, R.S. Klein, D.H. Hollenberg, J.J. Fox, Carbohydr. Res. 39 (1975) 227. (d) H. Tsutsumi, Y. Kawai, Y. Ishido, Carbohydr. Res. 73 (1979) 293.
[37] (a) ADF 2.01–2.2 Theoretical Chemistry, Vrije Universiteit Amsterdam. (b) E.J. Baerends, D.E. Ellis, P. Ros, Chem. Phys. 2 (1973) 41. (c) G. te Velde, E.J. Baerends, J. Comp. Phys. 99 (1992) 84. (d) C. Fonseca Guerra, METECC-95 (1995) 305.
[38] S.H. Vosko, L. Wilk, M. Nusair, Can. J. Phys. 58 (1980) 1200.
[39] A.D. Becke, Phys. Rev. A 38 (1988) 3098.
[40] J.P. Perdew, Phys. Rev. B 33 (1986) 8822.
[41] CERIUS2, version 3.5, Molecular Simulations INC., 1997.
[42] (a) L.A. Castonguay, A.K. Rappe, J. Am. Chem. Soc. 114 (1992) 583. (b) A.K. Rappe, C.J. Casewit, K.S. Colwell, W.A. Goddard-III, W.M. Skiff, J. Am. Chem. Soc.114 (1992) 10024. (c) A.K. Rappe, K.S. Colwell, Inorg. Chem. 32 (1993) 3438.
[43] A.K. Rappe, C.J. Casewit, W.A. Goddard-III, J. Phys. Chem. 95 (1991) 3358.
[44] F.W. Biegler-König, R.F.W. Bader, T.H. Tang, J. Comp. Chem. 3 (1982) 317.
[45] Xaim software developed by J.C. Ortiz, C. Bo, Universitat Rovira i Virgili, Tarragona, 1998.